Direct coupling of a laser-written photonic integrated circuit to a SPAD array

Giulio Gualandi[1,2], Simone Atzeni[2], Marco Gardina[2], Antonino Caime[1], Giacomo Corrielli[2], Ivan Labanca[3], Angelo Gulinatti[3], Roberto Osellame[2], Giulia Acconcia[3] and Francesco Ceccarelli[2,*]

[1] Dipartimento di Fisica - Politecnico di Milano, p.za L. da Vinci 32, 20133 Milan, 20133 Italy
[2] Istituto di Fotonica e Nanotecnologie - Consiglio Nazionale delle Ricerche, p.za L. da Vinci 32, Milan, 20133 Italy
[3] Dipartimento di Elettronica, Informazione e Bioingegneria - Politecnico di Milano, p.za L. da Vinci 32, Milan, 20133 Italy

Abstract

To date, several experiments in integrated quantum photonics exploit single-photon detectors operating at cryogenic temperatures coupled to photonic integrated circuits (PICs) through single-mode optical fibers. In this scenario, the complexity of the detection part represents an obstacle for the scalability of the entire setup. Here, we propose an alternative approach in which a programmable PIC fabricated by femtosecond laser writing (FLW) is interfaced directly to a silicon single-photon avalanche diode (SPAD) array. Each of the two components is realized by taking advantage of fully custom technologies able to provide state-of-the-art performance to the final application. The effectiveness of this solution is preliminary demonstrated by measuring a coupling efficiency as high as 93.2%, along with a system detection efficiency of 36.3% at 561 nm. These values, which are best in class, have the potential to unlock a new perspective in terms of scalability in quantum photonics experiments.

Introduction

Integrating manipulation and detection into a single device is paramount to advance the scalability of quantum photonic systems [1]. However, the monolithic integration is still a daunting task due to the different materials and technologies required to obtain state-of-the-art performance in each part. As a result, several experiments are still based on the optical coupling of a photonic integrated circuit (PIC) to off-chip superconducting single-photon detectors, whose cost, footprint and power consumption often represent a limit to the scalability. Furthermore, the optical coupling is typically made through single-mode fiber arrays, whose geometry constrains the waveguide arrangement at the output of the PIC [2].

In this work, we propose and report on a solution to this problem based on the direct coupling of a programmable PIC, fabricated by femtosecond laser writing (FLW) of waveguides in glass [3], to a single-photon avalanche diode (SPAD) array, manufactured in a planar silicon technology [4]. Preliminary results show a coupling efficiency (CE) as high as 93.2%, along with a system detection efficiency (SDE) of 36.3% at 561 nm, which are record values for direct waveguide-to-SPAD coupling.

*Correspondence to: francesco.ceccarelli@cnr.it

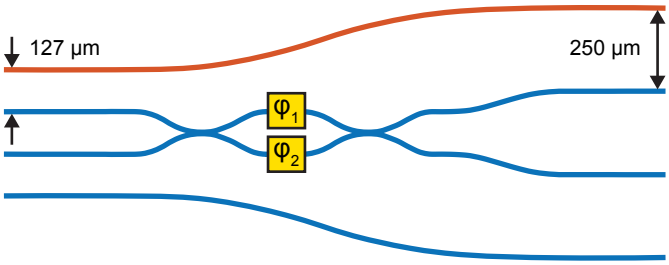

Fig. 1: Schematic layout of the programmable FLW-PIC designed to study the direct coupling with the SPAD array. The waveguide in red is the one used in this preliminary experiment. The vertical dimensions are stretched with respect to the horizontal ones for sake of clarity.

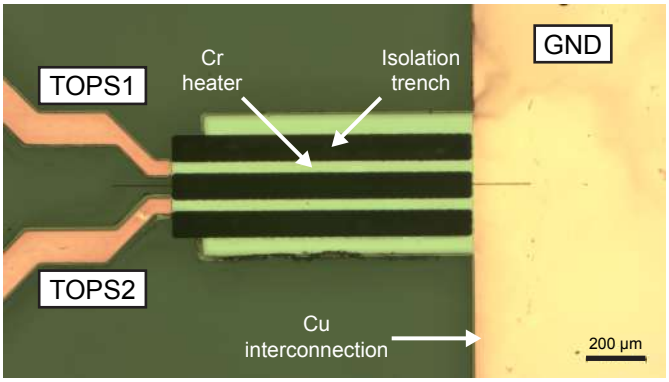

Fig. 2: Photomicrograph of the two thermo-optic phase shifters (TOPSs) fabricated on the two arms of the programmable MZI.

Design

The FLW-PIC layout (Fig. 1) is composed of 4 coplanar single-mode waveguides operating at 561 nm. The pitch at the input is 127 µm, to allow the coupling with a standard fiber array, and 250 µm at the output, to match the spacing of the SPAD pixels. The two lateral waveguides are independent, while the two central ones compose a programmable Mach-Zehnder interferometer (MZI). A thermo-optic phase shifter (TOPS), i.e. a resistive heater used to change the refractive index and thus route light at will, is realized on top of each arm of the MZI (Fig. 2). Two photolithograpic steps are employed to realize chromium heaters and copper interconnections. Thermal isolation trenches are fabricated at the sides of the heaters to reduce power dissipation and phase crosstalk, as required to use the programmable MZI as building block of universal photonic

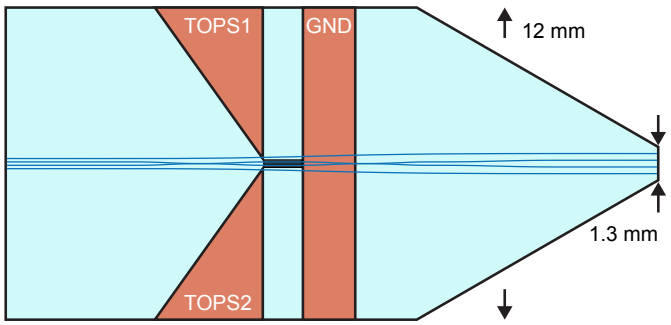

Fig. 3: Illustration of the die hosting the FLW-PIC. The chip is 25 mm long and 12 mm wide. The output is tapered down to 1.3 mm.

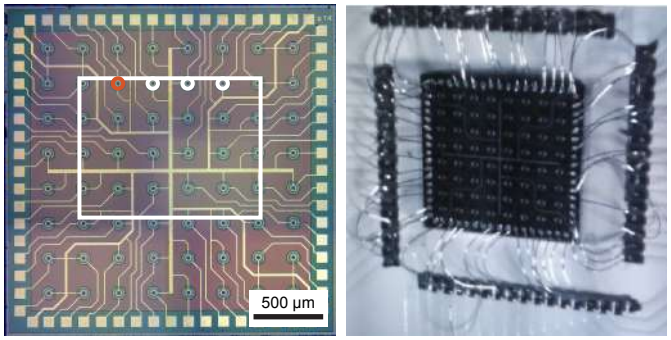

Fig. 4: (a) Photomicrograph of the SPAD array. The white rectangle highlights the FLW-PIC footprint ($1.3\times1\,\mathrm{mm}^2$). The white circles indicate the pixels chosen for the coupling. The red circle indicates the SPAD used in this preliminary experiment. (b) Photograph of the SPAD array taken from a camera used for the alignment.

processors [5]. The complete fabrication process is reported in [6]. Finally, the die is tapered by a dicing saw (Fig. 3) to avoid damages to the bonding wires surrounding the SPAD array.

The SPAD array [7] encompasses 64 pixels arranged in a 8×8 configuration (Fig. 4). Each detector has a circular active area with diameter of 20 µm and center-to-center spacing between adjacent pixels of 250 µm. The fabrication process chosen for the experiment is purposely optimized for detection of green light and for the minimization of noise sources like dark and crosstalk counts. The SPAD array is mounted on a detection module in which the same bias voltage is applied to all the cathodes through a common terminal, while each anode is routed to an individual bonding pad for connection to external active quenching circuits (AQCs) through wire-bonding. The AQCs [8] are arranged in a single chip containing 16 fully independent channels, 4 of which are chosen for the optical coupling (Fig. 4). The outputs of the selected AQCs, each providing a voltage pulse synchronous with the detection of a photon by the corresponding SPAD, are buffered through an on-board circuit and made available by SMA connectors.

Experimental results

In order to demonstrate the effectiveness and, thus, the potential of the combination of these two technologies, here we preliminary show the result of the direct coupling between a lateral waveguide (Fig. 1) and a SPAD pixel (Fig. 4). Thanks

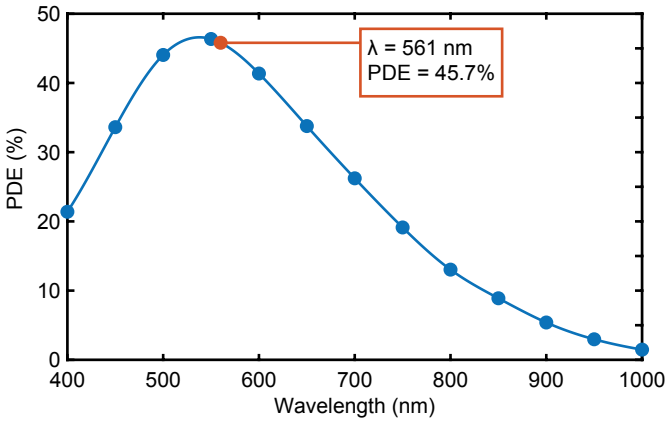

Fig. 5: PDE of the SPAD selected for the characterization of CE and SDE, measured through a standard free-space setup. The value for the operating wavelength is highlighted in red.

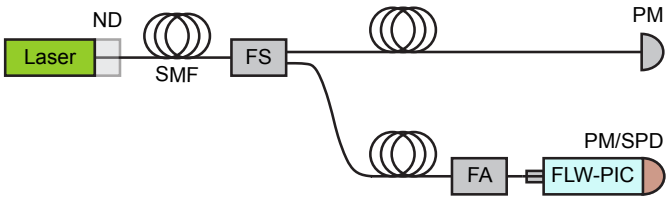

Fig. 6: Schematic of the experimental setup employed for the characterization of CE and SDE (ND = neutral density filter, SMF = single-mode fiber, FS = fiber splitter, FA = fiber attenuator, PM = power meter, SPD = SPAD array).

to the fine optimization of the FLW process, propagation losses are as low as $0.11\,\mathrm{dB\,cm^{-1}}$. As a result, the transmission for this waveguide after the fiber pigtailing is as high as T = 85.1%. The photon detection efficiency (PDE) of the SPAD measured with a standard free-space setup is reported in Fig. 5 for a 5 V excess voltage. A PDE = 45.7% is measured at 561 nm.

To characterize the CE introduced by the direct coupling and, thus, the overall SDE, we adapt the setup reported in [9] into the one depicted in Fig. 6. A laser beam at 561 nm is fiber coupled and subsequently split in half by a fiber splitter. One part is monitored by an auxiliary power meter, while the other beam, after being highly attenuated, is sent to the input fiber of the device. Firstly, we perform a calibration of the monitor in which the light intensity at the output of the FLW-PIC is measured through a second power meter. Secondly, the latter power meter is replaced by the SPAD module and the single-photon level is achieved by introducing a neutral density filter at the output of the laser. Then, we use a hexapod nanopositioner to actively align the SPAD by using real-time feedback from the measured count rate. A photograph of the assembled system is reported in Fig. 7. Once the count rate is maximum, we sweep the laser intensity to retrieve the linearity curve of the SPAD, i.e. the count rate n_{det} as a function of the photon rate n_{out} at the output of the FLW-PIC (Fig. 8), calculated according to the monitor. By extracting the best linear coefficient from this dataset we are able to estimate a product CE · PDE = 42.6±0.4% and, in turn, to isolate CE = 93.2±0.8% and to calculate an overall SDE = T · CE · PDE = 36.3±0.7%. The offset (background + dark counts) is measured separately.

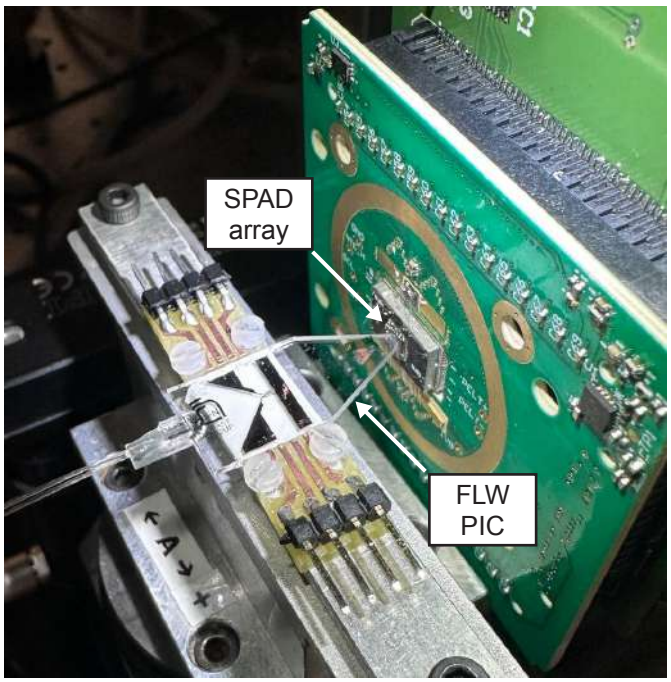

Fig. 7: Photograph showing the programmable FLW-PIC coupled to the SPAD array. The FLW-PIC is equipped with a fiber array at the input and electrical connectors at the sides. The SPAD array is mounted on a detection module along with all the auxiliary electronics.

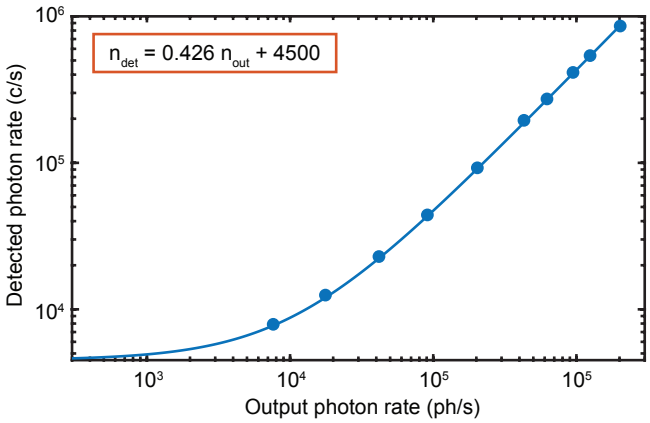

Fig. 8: Linearity of the SPAD selected for the characterization of CE and SDE. The result of the best linear fit is reported in the red box.

Conclusion

In this paper, we reported on the direct coupling of a programmable FLW-PIC to a silicon SPAD array. In particular, we showed a CE = 93.2% for a waveguide and a SPAD pixel, corresponding to a SDE = 36.3%. To our knowledge, these values are the highest among the SPADs integrated/assembled with PICs [10, 11, 12, 13]. For visible photons, our SDE is also comparable or even higher than the one reported for waveguide-integrated superconducting detectors [14], thus supporting the effectiveness of a hybrid approach based on independent technologies. As a matter of fact, both our platforms currently provide excellent performances thanks to two custom fabrication processes optimized independently and, notably, our coupling procedure does not introduce any constraints on them.

The developments unlocked by this work are manifold. After studying the programmable MZI coupled with two SPADs at the same time, interesting directions range from testing thicker SPAD arrays [15], in order to increase the SDE, to exploiting the unique 3D capabilities of the FLW technology, in order to couple programmable 3D FLW-PIC [2] and 2D SPAD arrays. If successful, both developments would have a remarkable impact on the scalability of quantum photonics experiments.

References

[1] J. Wang et al. Integrated photonic quantum technologies. *Nat. Photonics*, 14(5):273–284, 2020.

[2] F. Hoch et al. Reconfigurable continuously-coupled 3D photonic circuit for boson sampling experiments. *npj Quantum Inf.*, 8(1):55, 2022.

[3] G. Corrielli et al. Femtosecond laser micromachining for integrated quantum photonics. *Nanophotonics*, 10(15):3789–3812, 2021.

[4] M. Ghioni et al. Progress in silicon single-photon avalanche diodes. *IEEE J. Sel. Top. Quantum Electron.*, 13(4):852–862, 2007.

[5] N. C. Harris et al. Linear programmable nanophotonic processors. *Optica*, 5(12):1623–1631, 2018.

[6] R. Albiero et al. Toward higher integration density in femtosecond-laser-written programmable photonic circuits. *Micromachines*, 13(7):1145, 2022.

[7] F. Ceccarelli et al. Gigacount/second photon detection module based on an 8×8 single-photon avalanche diode array. *IEEE Photonics Technol. Lett.*, 28(9):1002–1005, 2016.

[8] G. Acconcia et al. High-voltage integrated active quenching circuit for single photon count rate up to 80 Mcounts/s. *Opt. Express*, 24(16):17819–17831, 2016.

[9] T. Gerrits et al. Calibration of free-space and fiber-coupled single-photon detectors. *Metrologia*, 57(1):015002, 2020.

[10] A. Trenti et al. On-chip quantum communication devices. *J. Light. Technol.*, 40(23):7485–7497, 2022.

[11] F. Acerbi et al. Monolithically integrated SiON photonic circuit and silicon single-photon detectors for NIR-range operation. *J. Light. Technol.*, 2023.

[12] N. J. D. Martinez et al. Single photon detection in a waveguide-coupled Ge-on-Si lateral avalanche photodiode. *Opt. Express*, 25(14):16130–16139, 2017.

[13] J. Zhang et al. Hybrid and heterogeneous photonic integrated near-infrared InGaAs/InAlAs single-photon avalanche diode. *Quantum Sci. Technol.*, 8(2):025009, 2023.

[14] M. A. Wolff et al. Broadband waveguide-integrated superconducting single-photon detectors with high system detection efficiency. *Appl. Phys. Lett.*, 118(15):154004, 2021.

[15] A. Gulinatti et al. Custom silicon technology for SPAD-arrays with red-enhanced sensitivity and low timing jitter. *Opt. Express*, 29(3):4559–4581, 2021.